Tunable Photoluminescence of Closed-Shell Heterobimetallic Au−Ag Dicyanide Layered Systems

**Julie Clarissa F. Colis,[§] Christie Larochelle,[¶] Eduardo J. Fernández,[‡]
José M. López-de-Luzuriaga,[‡] Miguel Monge,[‡] Antonio Laguna,[†] Carl Tripp,[§,||] and
Howard Patterson*,[§]**

*Department of Chemistry and Laboratory for Surface Science and Technology, University of Maine,
Orono, Maine 04469, Department of Physics, Franklin & Marshall College, Lancaster, Pennsylvania 17604,
Departamento de Química, Universidad de La Rioja, Logroño, La Rioja, Spain, and Departamento de Química
Inorganica, Universidad de Zaragoza, Zaragoza, Spain*

The excited-state properties of the layered $La[Ag(CN)_2]_3$ and $La[Au(CN)_2]_3$ systems have been examined and compared with mixed-metal systems of varying metal ratios such as $La[Ag_{0.78}Au_{0.22}(CN)_2]_3$, $La[Ag_{0.55}$-$Au_{0.45}(CN)_2]_3$, $La[Ag_{0.33}Au_{0.67}(CN)_2]_3$, and $La[Ag_{0.19}Au_{0.81}(CN)_2]_3$. We have found that these mixed-metal systems luminesce quite strongly at room temperature at an energy that is tunable and depends on the Au:Ag stoichiometric ratio. The emission energy of the mixed-metal samples lies between those of the pure Au and Ag systems. This provides evidence that the excited states responsible for this emission are delocalized over the Ag and Au centers. The strong luminescence of the mixed-metal systems at ambient temperatures is in stark contrast to the weak luminescence behavior of pure $La[Au(CN)_2]_3$ and $La[Ag(CN)_2]_3$ samples, which makes the mixed-metal systems more viable than the pure systems for practical applications.

Introduction

The study of formally closed-shell d^{10} metal ions such as gold-(I) has continued to attract our attention. Bonding interaction is not expected between two closed-shell metal ions with an $nd^{10}(n+1)s^0$ electronic configuration; however, results of extensive experimental and theoretical studies reveal that weak bonding exists between two gold(I) atoms at a separation of less than 3.5 Å.[1,2] This gold−gold aggregation has been termed aurophilicity. In a similar fashion, there also exist argentophilic interactions, although these have been reported and calculated to be weaker than gold−gold interactions.[3−5] Our group has reported a comparison between Au−Au and Ag−Ag interactions in the ground and excited states of dicyano complexes.[6] These studies of cyano complexes of Au(I) and Ag(I) relate the photoluminescence properties of the systems to the formation of metal−metal bonded excimers and exciplexes. The optical phenomenon of "exciplex" tuning has been found to be a characteristic property of dicyanoargentate and dicyanoaurate compounds. Emission energies of these systems can be tuned by varying certain physical parameters such as temperature,[7] pressure,[8] excitation wavelength,[9] and dopant concentration.[9b,10] Tuning the excited-state properties is extremely important in a variety of optoelectronic applications in relation to some fundamental scientific issues such as excitonic energy transfer and the development of new photonic devices.[11−13]

The rich optical properties of the d^{10} gold and silver metals have prompted our group to extend investigations to mixed-metal systems. We combine together the dicyanoaurate and dicyanoargentate ions to come up with a novel system with the expectation that it would exhibit the interesting properties of the pure systems and would have unique properties of its own as well. There have been few studies[3,14−18] reported on hetero-bimetallic molecular assemblies with the overall structure strongly influenced by the Au−Au interactions. Ag(I) centers have also been used as a design element in the synthesis of supramolecular structures.[19] Cyanometalate anions have been used as building blocks in supramolecular coordination polymers because of their ability to form strong bonds with transition metal cations.[20−22] It is important to note that, for the above-mentioned heterometallic systems, interaction is just between the same metals. Although interestingly, in the [Cu(en)Cu-$(CN)_2Ag(CN)_2$] complex a Cu(I)−Ag(I) interaction has been found to help stabilize the assembly.[19] In this paper, we report results of Ag(I) −Au(I) interaction for the samples $La[Ag_xAu_{1−x}$-$(CN)_2]_3$ with $x = 0.78$, 0.55, 0.33, and 0.19. The results from these samples are similar to those obtained for a series of quasi-one-dimensional mixed Pt−Pd and Pt−Ni tetracyanide systems studied. For example, for $Ba[Pt_xNi_{1−x}(CN)_4]·nH_2O$ ($x = 0−1$) pellet absorption measurements give the change in energy of the electronic states versus x, which have been assigned to mixed-metal delocalized electronic states.

In this paper we report the results of our studies on $La[Ag-(CN)_2]_3$ and $La[Au(CN)_2]_3$ with the extension of the study to closed-shell d^{10} heteroatomic metal donor lanthanide ion complexes {$La[Ag_xAu_{1−x}(CN)_2]_3$, $x = 0.78$, 0.55, 0.33, and 0.19}. The Au−Ag mixed-metal complexes exhibit many of the desirable properties of the pure dicyanoaurate and dicyanoargentate species, one of which is tunability. Furthermore, the complexes have been found to luminesce quite strongly at room temperature, a property which is not possessed by the pure samples. The studies therefore aim to characterize the pure gold and silver cases as well as the mixed-metal gold−silver dicyanides and explain their interesting properties.

[§] Department of Chemistry, University of Maine.
[¶] Franklin & Marshall College.
[‡] Universidad de La Rioja, Logroño.
[†] Universidad de Zaragoza.
[||] Laboratory for Surface Science and Technology, University of Maine.

TABLE 1: Computed Au:Ag Ratio in the Mixed-Metal Lanthanide Ion Single Crystals

mother solution	computed loading based on Raman measurements	empirical formula from X-ray studies
$La[Ag(CN)_2]_3$		$La[Ag(CN)_2]_3 \cdot 3H_2O$
$La[Ag_{0.90}Au_{0.10}(CN)_2]_3$	$La[Ag_{0.79}Au_{0.21}(CN)_2]_3$	$La[Ag_{0.78}Au_{0.22}(CN)_2]_3 \cdot 3H_2O$
$La[Ag_{0.75}Au_{0.25}(CN)_2]_3$	$La[Ag_{0.55}Au_{0.45}(CN)_2]_3$	
$La[Ag_{0.50}Au_{0.50}(CN)_2]_3$	$La[Ag_{0.35}Au_{0.65}(CN)_2]_3$	$La[Ag_{0.33}Au_{0.67}(CN)_2]_3 \cdot 3H_2O$
$La[Ag_{0.25}Au_{0.75}(CN)_2]_3$	$La[Ag_{0.19}Au_{0.81}(CN)_2]_3$	
$La[Au(CN)_2]_3$		$La[Au(CN)_2]_3 \cdot 3H_2O$

Experimental Section

Synthesis. All reagents were obtained commercially and used as received. Crystals were grown in 1% agar gel solutions in U-tubes. The agar gel solution was deposited on the bottom of the U-tubes. Stoichiometric solutions of the appropriate KM-$(CN)_2$ (M = Ag, Au) and $La(NO_3)_3$ were then layered above the gel on opposite sides of the tubes. The aqueous solutions of the host $KM(CN)_2$ and the dopant $La(NO_3)_3$ were allowed to diffuse toward each other through the gel medium. Crystals formed in the gel and were then collected.

Raman Studies. Raman spectra were recorded on a Renishaw Raman imaging microscope system 1000 equipped with a diode laser operating at $\lambda_{ex} = 785$ nm. The same single crystal was used for all Raman measurements.

Luminescence Studies. Steady-state photoluminescence spectra were collected using a Photon Technology International Model QuantaMaster-1046 spectrophotometer equipped with a 75 W xenon lamp. Wavelengths were selected with two excitation monochromators and a single emission monochromator. The instrument is interfaced with a computer, and software supplied by the manufacturer was used to collect and record data. All excitation spectra were corrected for spectral variations in the lamp using the quantum counter method. Luminescence spectra were recorded as a function of temperature using liquid nitrogen as the coolant in a Model LT-3-110 Heli-Tran cryogenic liquid transfer system equipped with a temperature controller.

Computational Details. The molecular structures used in the theoretical studies of $[La(H_2O)_3][M(CN)_2]_3$ (M = Ag and/or Au) were taken from the X-ray diffraction results for pure and mixed experimental compounds. Keeping all distances, angles, and dihedral angles frozen, single-point density functional theory (DFT) calculations were performed on the models. In both the single-point ground-state calculations and the subsequent calculations of the electronic excitation spectra, the default Beck–Perdew (B–P) functional[24–26] as implemented in TURBO-MOLE[27] was used. The excitation energies were obtained at the density functional level using the time-dependent perturbation theory approach (TD-DFT),[28–32] which is a density-functional-theory generalization of the Hartree–Fock linear response (HF-LR) or random-phase approximation (RPA) method.[33]

In all calculations, the Karlsruhe split-valence quality basis sets[34] augmented with polarization functions[35] were used (SVP). The Stuttgart effective core potentials in TURBOMOLE were used for Au, Ag, and La.[36] Calculations were performed assuming local symmetry C_{3v} for the Ag_3 model, C_s for the Ag_2-Au and $AgAu_2$ models, and C_3 for the Au_3 model system as obtained by the automatic symmetry recognition script implemented in TURBOMOLE.

Results and Discussion

Synthesis. Six lanthanide ion complexes were prepared: $La[Ag_xAu_{1-x}(CN)_2]_3$, $x = 1, 0.90, 0.75, 0.50, 0.25,$ and 0.

Hexagonally shaped, white crystals were harvested 3–10 days after preparation. It took a month longer to form the pure crystals, $La[Ag(CN)_2]_3$ and $La[Au(CN)_2]_3$. Crystals of the pure gold and silver systems and the mixed-metal crystals $La[Ag_{0.90}Au_{0.10}(CN)_2]_3$ and $La[Ag_{0.50}Au_{0.50}(CN)_2]_3$ (Ag/Au stoichiometric ratios from the precursors) were found to be suitable for X-ray studies. Empirical formulas computed from results of X-ray structure determination studies gave the Ag/Au loading in the crystals. Also, the Au/Ag ratio of the samples was computed by integrating the peak areas under the $\nu(CN)$, taken from Raman measurements of the $\nu(CN)$ stretching mode arising from $Ag(CN)_2^-$ compared to the peak area of the $\nu(CN)$ stretching mode arising from $Au(CN)_2^-$ for each sample. The computed values are in agreement with the Au/Ag ratio from X-ray studies (Table 1). Comparing the computed Au/Ag ratio for the single crystals of the mixed-metal lanthanide complex with that of the precursor, it is observed that there is higher loading of the gold ions versus that of the silver ions in the crystal formed compared to the Ag/Au ratio in the starting materials.

Crystal Structures. Crystal structures of four lanthanide complexes ($La[Au(CN)_2]_3 \cdot 3H_2O$, $La[Ag(CN)_2]_3 \cdot 3H_2O$, $La[Ag_{0.78}Au_{0.22}(CN)_2]_3 \cdot 3H_2O$, and $La[Ag_{0.33}Au_{0.67}(CN)_2]_3 \cdot 3H_2O$) have been solved. The detailed discussion of the crystal structures is presented in another paper.[37] These compounds have a layered structure which consists of alternating layers of $M(CN)_2^-$ (M = Ag, Au) and La^{3+} ions. The counterion, La^{3+} ion, in these compounds occupies a hexagonal hole and interacts with the N atom of the CN^- ligand. All the complexes belong to the hexagonal crystal system in the space group $P6_3/mcm$ (No. 193). Water molecules surround the La^{3+} ions. Figure 1 shows the packing diagram for $La[Ag_xAu_{1-x}(CN)_2]_3 \cdot 3H_2O$ as viewed down the a axis.

Raman Studies. Raman scattering experiments were carried out to complement structural studies on the characterization of the samples. The high- and low-frequency regions of the Raman spectra for the samples are shown in Figure 2a,b, respectively. Assignments of the Raman bands are given in Table 2. The Raman spectra of $La[Ag_xAu_{1-x}(CN)_2]_3$, $x = 0, 0.25, 0.50, 0.75, 0.90,$ and 1, systems can be conveniently discussed by analogy with the Raman spectra of $KAu(CN)_2$ and $KAg(CN)_2$, which have been studied in detail.[38–41] In $KAu(CN)_2$ Raman studies,[40–42] bands are observed at ~2160 cm^{-1} (CN stretch) and at ~305 cm^{-1} (AuCN bend). In a previous work,[40] the Au–C stretch has not been observed but has been assigned to be at 452 cm^{-1}, deduced from infrared combination bands. In the work of Adams and Fletcher,[41] the Au–C stretch has been reported although it was observed as an extremely weak and broad pair of bands at ca. 450 cm^{-1}. From a comparison to the literature, we assign bands for $La[Au(CN)_2]_3$ at 2172 and 2166 cm^{-1} to CN stretching modes and at 335 and 323 cm^{-1} to AuCN bending modes. A very weak Raman band was also observed at 459 cm^{-1}, which is assigned to the AuC stretching frequency. While symmetry considerations suggest that only one peak for the CN stretch is expected, two peaks are observed. The appearance of two peaks in the CN stretching region for $Au(CN)_2^-$-containing complexes

Au−Ag Dicyanide Layered System Photoluminescence

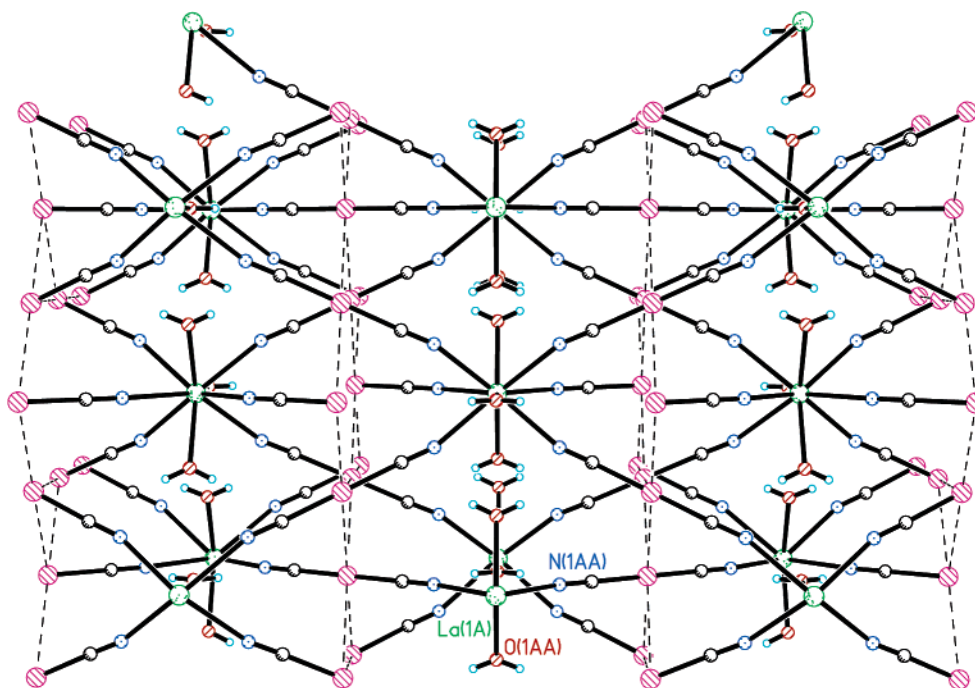*J. Phys. Chem. B, Vol. 109, No. 10, 2005* **4319**

Figure 1. One La^{3+} atom layer with water molecules coordinated with respect to the whole structure. Large striped pink circles represent Ag or Au atoms, large hatched green La atoms, small black C atoms, small blue N atoms, small striped orange O atoms, and small blue-green H atoms. Dotted lines represent possible M···M interactions.

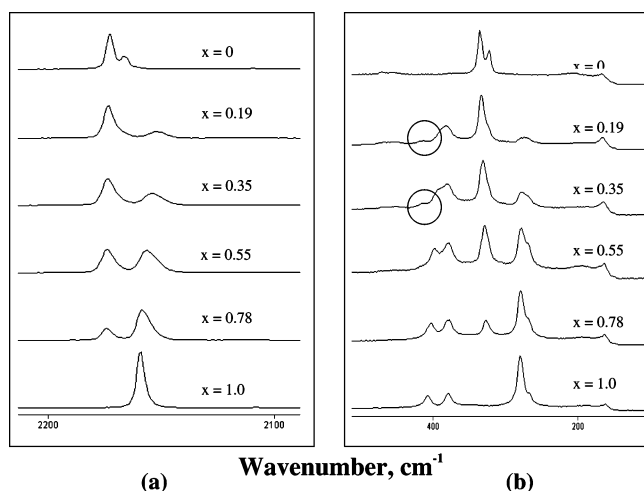**Figure 2.** Raman shifts of La[Ag$_x$Au$_{1-x}$(CN)$_2$]$_3$, (a) C−N stretching frequency and (b) M−CN bending and M−C stretching region. Experimental conditions: laser excitation of 785 nm at 298 K.

have been previously reported.[40−42] A possible explanation would be that a new complex is formed arising from the interaction of Au(CN)$_2$$^-$ with the cation. This was the suggested explanation for the appearance of a shoulder in the peak due to the ν(CN) stretch upon an increase of the LiAu(CN)$_2$ concentration from 1 to 5 M. However, we believe that, in the case of La[Au(CN)$_2$]$_3$, a more plausible explanation for the presence of two peaks due to the CN stretch would be the presence of two or more nonequivalent Au(CN)$_2$$^-$ molecular sites. This has been the case for the TlAu(CN)$_2$ complex wherein four separate transitions in the CN stretching region have been observed.

In KAg(CN)$_2$ Raman studies,[38−41] fundamental bands are observed at ∼2140 cm^{-1} (CN stretch), and at ∼250 cm^{-1} (AgCN bend). Analogous to KAu(CN)$_2$, the Ag−C stretching frequency has been reported[39,40] to be absent or extremely low in intensity. The Ag−C stretch has been assigned to be at ∼360

cm^{-1}, deduced from infrared-active combination bands.[39] Our measurements show that the La[Ag(CN)$_2$]$_3$ fundamental bands are at 2159 cm^{-1} (CN stretch) and at 280 cm^{-1}, 266 cm^{-1} (AgCN bend). Two well-resolved peaks are observed at 407 and 379 cm^{-1}, which we assign as AgC stretching frequencies.

It is important to note that in the current studies all the Au-(I)-based Raman stretching and bending frequencies are consistently found to have higher frequencies than the Ag(I)-based Raman peaks. This is supported by the work of Jones and others.[40] Also, the relative Au−C and Ag−C bond lengths must be considered. In a structural report on these systems[37] the Au−C bond length (1.994(14) Å) was found to be shorter than the Ag−C bond length (2.059(3) Å). Che et al.[40] in their paper on studies of [M$_2$(μ-dcpm)2]$^{2+}$ (M = Ag, Au) reported the force constant, assuming a pure M$_2$ stretch mode, to be 0.203 mdyn Å^{-1} for F(Ag$_2$) and 0.449 mdyn Å^{-1} for F(Au$_2$). Jones reported[40] the force constant, K(MC) for [Au(CN)$_2$]$^-$ to be 2.745 mdyn Å^{-1} and for [Ag(CN)$_2$]$^-$ to be 1.826 mdyn Å^{-1}. Therefore, the bond strength of Ag−Ag versus Au−Au interactions has a significant influence on the position of the frequency bands.

It was observed that there is a correlation between the relative intensities of the respective peaks from the ν(CN) stretching mode arising from Ag(CN)$_2$$^-$ and Au(CN)$_2$$^-$ ions to the Ag and Au loading in the sample. In fact, as mentioned earlier, the Ag/Au ratios in the mixed-metal samples were computed by integration of the peak areas of the ν(CN) stretching mode arising from Ag(CN)$_2$$^-$ and Au(CN)$_2$$^-$ ions for each sample. This method afforded a faster way to determine the Ag/Au ratio in the final product rather than have the crystal structure of each sample solved. Upon comparison to the empirical formulas resolved from X-ray studies of two mixed crystals, La[Ag$_{0.90}$-Au$_{0.10}$(CN)$_2$]$_3$ and La[Ag$_{0.50}$Au$_{0.50}$(CN)$_2$]$_3$, it was found that the Ag/Au ratio solved from Raman data are in agreement with the X-ray determined empirical formulas. The Raman data therefore provided information on the Ag/Au loading in the other

TABLE 2: Assignment of Raman Bands/Wavenumber, cm^{-1}

La[Ag(CN)$_2$]$_3$	La[Ag$_{0.78}$Au$_{0.22}$(CN)$_2$]$_3$	La[Ag$_{0.55}$Au$_{0.45}$(CN)$_2$]$_3$	La[Ag$_{0.33}$Au$_{0.67}$(CN)$_2$]$_3$	La[Ag$_{0.19}$Au$_{0.81}$(CN)$_2$]$_3$	La[Au(CN)$_2$]$_3$	assgnmt
2159.2	2158.4	2156.1	2153.9	2151.7		ν(CN)
—	2174.1	2174.0	2173.6	2173.2	2172.6	ν(CN)
					2166.3	
—	—	—	459.37	459.37	459.37	ν(AuC)
406.81	403.06	397.06	393.47	—	—	ν(AgC)
378.89	378.89	378.89	380.55	382.64		
	327.21	329.29	331.37	333.87	335.54	δ(AuCN)
					323.04	
279.69	279.69	278.44	277.19	273.2	—	δ(AgCN)
265.94	268.86	268.44	270.11			

crystal systems whose structures were not solved by X-ray studies.

The Raman measurements provide additional evidence for the presence of mixed-metal Au−Ag clusters. It is with the ν-(AgC) and ν(AuC) modes that the influence of the silver−gold interaction is detected. Figure 2b shows the low-energy Raman shifts of pure La[Ag(CN)$_2$]$_3$ (bottom) and La[Au(CN)$_2$]$_3$ (top) with the mixed-metal complexes at decreasing silver content in between. The two bands at ∼400 cm^{-1} are assigned to ν-(AgC), while the very weak band at ∼460 cm^{-1} to ν(AuC). As the Ag loading is decreased, a new band (encircled in Figure 2b) emerges which appears between the bands arising from ν-(AgC) and ν(AuC) modes, at ∼410 cm^{-1}. This we believe is due to the presence of the mixed-metal Ag−Au clusters. The ν(AgC) is affected by the presence of Au ions in the system, and the perturbation causes broadening of the two sharp bands and onto becoming a single peak. This provides further evidence that there are Ag−Au species present. In the Raman spectra (second from bottom, Figure 2b), the two bands assigned to ν(AgC) are still distinct, although a peak in the middle of the two bands is shown to be emerging. The other bands in the low-energy region of the Raman spectra are assigned as follows: a bending mode, δ(AuCN) at ∼330 cm^{-1}; and at ∼270 cm^{-1}, δ(AgCN). The change in relative intensities of the bands arising from δ(AgCN) and δ(AuCN) is consistent with the Ag and Au loading in the mixed-metal complexes, respectively.

Luminescence Studies. Luminescence experiments were carried out on all the La complexes.[43] Figure 3a shows the emission spectra of La[Ag(CN)$_2$]$_3$ for different excitation wavelengths. The spectra show that there is tunability of La-[Ag(CN)$_2$]$_3$ by site-selective excitation. From the spectra four emission peaks are observed: 322, 347, 400, and 470 nm. On the basis of lifetime measurements,[43a] the higher emission bands at 322 and 347 nm are assigned to ^{1}MC and ^{3}MC states, respectively. The less intense bands at lower energies are assigned to emissions arising from excitons trapped in the cluster defect sites in the crystal system.[44] Different excitation wavelengths result in emission from different cluster defects. It has been observed that tunability of emission spectra in La[Ag-(CN)$_2$]$_3$ can also be achieved by varying the temperature. Steady-state luminescence spectra of La[Ag(CN)$_2$]$_3$ are shown in Figure 3b, at both room temperature and 77 K. At room temperature only one peak at 345 nm is observed, but when the temperature is decreased another peak at 470 nm is observed.

In La[Au(CN)$_2$]$_3$ single crystals, upon excitation at 310 nm, two emission peaks are observed at 431 and 493 nm. Lifetime measurements[43a] have allowed us to assign the bands to ^{1}MC and ^{3}MC states, respectively. Tunability by site-selective excitation is observed with different emission peaks observed upon excitation at different wavelengths, as shown in Figure 4a. The appearance of the different emission peaks we believe are due to the presence of different cluster sizes of aurophilic−argentophilic linked oligomers. Eisenberg et al. has also reported
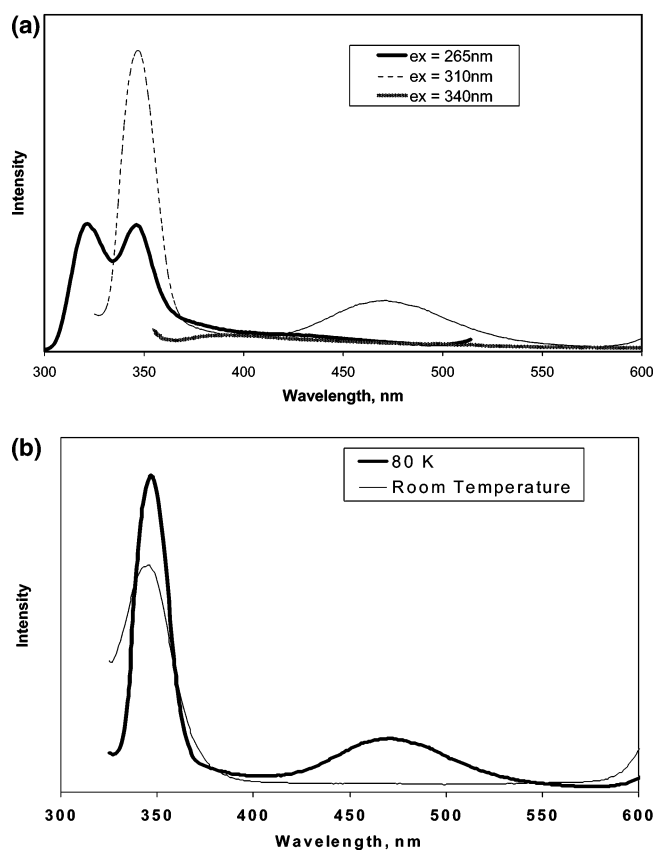

Figure 3. (a) Emission spectra for La[Ag(CN)$_2$]$_3$ single crystals at 80 K for a variety of excitation wavelengths and (b) room and liquid nitrogen temperatures with λ_{ex} = 310 nm.

this occurrence in gold complexes in frozen glass media.[45] Upon cooling the sample to 77 K from room temperature, a significant red shifting of the emission bands has been observed, as shown in Figure 4b. Au−Au distances shorten at lower temperatures,[46] thereby increasing the gold−gold interaction. This fact indicates that the gold−gold distance has a significant influence on the HOMO−LUMO gap which decreases with decreasing Au−Au separation. The increased interaction at low temperatures promotes orbital mixing and, hence, a decreased emission energy.

Four mixed-metal samples, La[Ag$_{0.78}$Au$_{0.22}$(CN)$_2$]$_3$, La[Ag$_{0.55}$Au$_{0.45}$(CN)$_2$]$_3$, La[Ag$_{0.33}$Au$_{0.67}$(CN)$_2$]$_3$, and La[Ag$_{0.19}$Au$_{0.81}$(CN)$_2$]$_3$, were prepared. Figure 5 shows the emission spectra of the lanthanum gold and silver pure samples and the mixed-metal compounds, at a fixed excitation wavelength of 265 nm. Note that the emission spectra of the mixed-metal systems lie between that of the pure Ag and Au systems. The maximum peak positions of the mixed-metal systems, respectively, show a trend of leaning to the Ag or Au peak position depending on the loading. This shows that the emission energy can also be
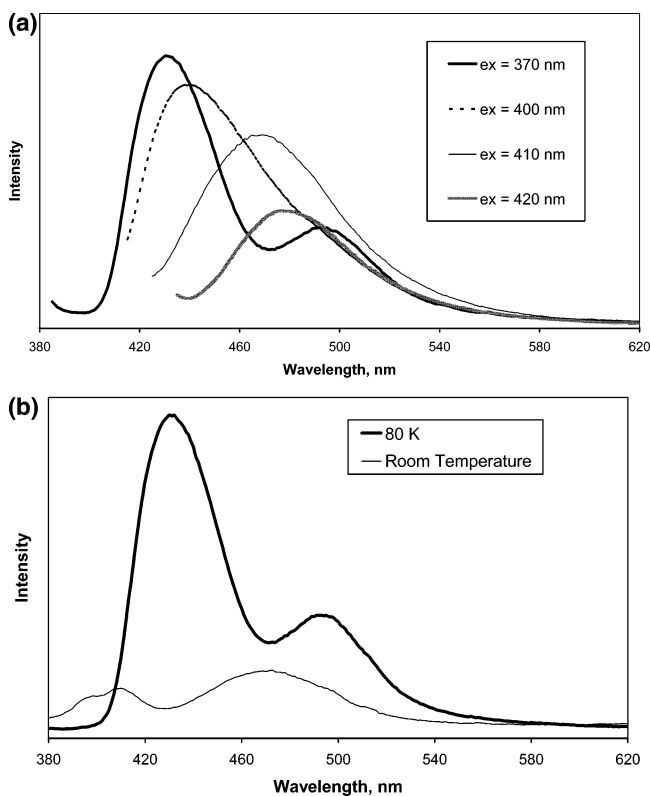
Au−Ag Dicyanide Layered System Photoluminescence

J. Phys. Chem. B, Vol. 109, No. 10, 2005 **4321**

(a)

(b)

Figure 4. (a) Emission spectra for La[Au(CN)$_2$]$_3$ single crystals at 80 K for a variety of excitation wavelengths and (b) variable temperatures with λ_{ex} = 340 nm.

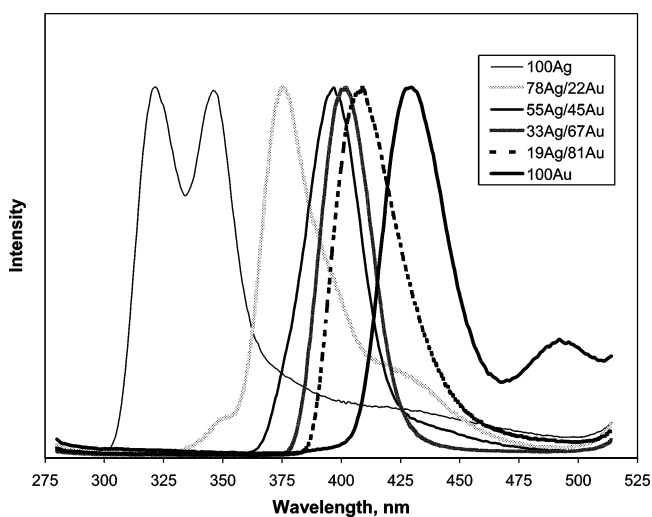**Figure 5.** Emission spectra for La[Ag$_x$Au$_{1-x}$(CN)$_2$]$_3$ donor species at 80 K with λ_{em} = 265 nm.

tuned by varying the ratio of the Ag/Au. The emission profiles of the mixed-metal compounds are different from the pure samples since they show only one peak when excited at various excitation wavelengths. This we explain as due to the excited state delocalized over the Ag and Au centers. An exception to this is the case with La[Ag$_{0.78}$Au$_{0.22}$(CN)$_2$]$_3$, which shows shoulders at ∼350 and ∼428 nm. The sample has a high silver loading; hence the profile of the spectra is more similar to La-[Ag(CN)$_2$]$_3$. It should be pointed out that because of the isostructuralism of the mixed and pure samples, we do not have symmetry breaking. In all the structures Au/Ag are lying on an inversion center.

DFT and TD-DFT Calculations. We have carried out DFT and TD-DFT calculations in order to explain some of the striking
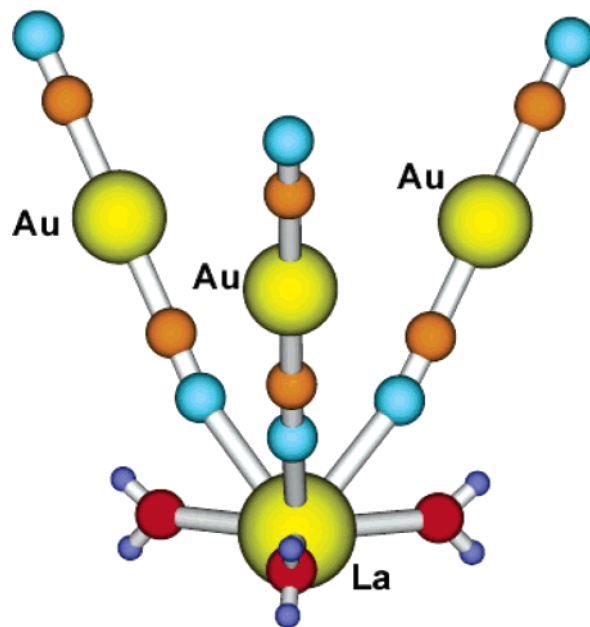

Figure 6. Theoretical model system [La(H$_2$O)$_3$][Au(CN)$_2$]$_3$ representing the pure La(III)−Au(I) system.

photophysical features of the La[M(CN)$_2$]$_3$ (M = Ag and/or Au) pure and mixed systems. The aim of these calculations is the study of the molecular orbitals (MO's) and the population analysis to check the contribution of each atom to the occupied and virtual orbitals. Indeed, the use of the TD-DFT calculations permits one to obtain information about the theoretical absorption spectra of simplified model systems based on the X-ray diffraction structures obtained for the pure and mixed La-[M(CN)$_2$]$_3$ systems. These theoretically obtained absorption spectra can be compared among them and also with the experimental results. For this, we have built up four different trinuclear (based on gold and silver atoms) theoretical models that would represent the different Ag:Au ratios (3:0, 2:1, 1:2, and 0:3) obtained experimentally (see Figure 6 for the pure Au$_3$ model system). We have considered that these models would represent fairly well the experimental structures because they correspond to a stoichiometry whose repetition units give rise to the extended crystal structures for the pure gold and silver systems and on the other hand are approximate to some experimental units for the mixed-metal ones.

Single-point DFT calculations for the pure Ag(I) and Au(I) model systems display similar trends regarding the population analysis for the occupied and the virtual orbitals. Thus, the highest occupied molecular orbitals are mainly metal (Ag(I) or Au(I)) and ligand (CN$^-$)-based (see Tables S1 and S2 of the Supporting Information for the population analysis), while the lowest empty orbitals are mainly based on the La(III) ions, although some contributions from the CN$^-$ ligands and especially from gold and silver centers would be important for the emissive properties arising from metal-centered transitions (see experimental assignment).

The mixed model containing two silver(I) and one Au(I) center (Ag$_2$Au) shows for the highest occupied molecular orbitals an important Ag(I) and CN$^-$ character with some contributions from Au(I) centers. An analogous trend is obtained for the mixed Au$_2$Ag model system but with a higher Au(I) and CN$^-$ character and some contribution from the Ag(I) center. Lanthanum ions and water molecules have almost no contribution to the highest occupied orbitals. On the other hand, La(III) ions are the main contribution to the lowest empty molecular

orbitals. Nevertheless, as in the pure systems and in accord with the experimental results some contributions from the Au(I) and Ag(I) centers are likely to be important in terms of the luminescent properties of these systems (see Tables S3 and S4 of the Supporting Information for the results of the population analyses performed on the mixed-model systems).

After the analysis of the electronic structure on the four theoretical model systems, we have carried out TD-DFT calculations in order to obtain the first few singlet electronic excitations for each of them. We cannot presently estimate the strength, given by spin−orbit effects, to the triplet transitions. If we first have a look at the energies and intensities of the calculated theoretical transitions, we can discuss some interesting features compared to the experimental photophysical properties. As in the luminescence measurements, the theoretical energy absorption is directly related to the amount of silver(I) ions in the systems. Thus, while the pure Ag(I) system shows the higher energy absorption, when we decrease the silver loading, the theoretical absorption profiles appear at lower energy values for Ag_2Au and $AgAu_2$ models, with the pure Au(I) model (no Ag(I) content) being the one that displays the lowest energy absorption (see Supporting Information). Another interesting feature in the difference between the pure and the mixed systems is the different intensity of luminescent emission. Thus, it has been experimentally observed that the intensity of the luminescence arising from the mixed Ag(I)−Au(I) systems is stronger than that of the pure Ag(I) or Au(I) systems. Previous TD-DFT calculations on chlorophyll *a* and pheophytin *a* show that the oscillator strength parameter can be used to compare the different theoretical intensities of the predicted absorption spectra for such a molecule.[47] In this sense, we have observed similar trends in the comparison of the theoretical absorption spectra for the pure and the mixed model systems. The pure Ag(I) and Au(I) model systems display similar oscillator strength values both at high and low energies, respectively. In the case of the theoretical absorption spectra for the mixed Ag_2Au and $AgAu_2$ models, it is important to note stronger oscillator strength values (almost double) than in the pure systems. This shows the same trend as the stronger luminescence intensity of the mixed systems versus the pure systems. Anyway, one should take into account that the relationship between experimental luminescence intensity and oscillator strength is not straightforward but also depends on the nonradiative rate. What we observe theoretically is just that a radiative transition is more likely in the mixed systems. Indeed, the increased intensity in the mixed-metal systems would be due to both oscillator strength values and to symmetry breaking. Anyway, in the pure Ag_3 model the oscillator strength values change very slightly by breaking the symmetry from C_{3v} to C_3 (see Supporting Information).

Regarding the molecular orbitals involved in the theoretical excitations we can make different observations depending on the different model systems. Thus, the most important theoretical transitions observed for the pure $La[Ag(CN)_2]_3$ or $La[Au(CN)_2]_3$ model systems involve silver (or gold)-based MOs and ligand (CN)-based MOs as occupied orbitals and arise to La(III)-based MOs with some contributions from the ligands and the Ag or Au centers, respectively. In this sense, we could assume a metal−ligand to metal charge transfer for the absorption spectra of the pure systems. On the other hand, taking into account the experimental assignment for the luminescent properties as metal-centered (^1MC and ^3MC) transitions, we would qualitatively explain this fact as a participation of the virtual orbitals 33a (pure gold model) and $27a_1$, 33e, $7a_2$, 34e, and 29e (pure silver

model) in the emissive properties in which a higher participation of the coinage metals is observed in the population analysis implying a delocalization over more than one metallic center.

The mixed Au(I)−Ag(I) systems display similar inital and final states for the theoretical transitions as in the pure systems. Thus, as in the pure systems, the most important contribution to the initial states are the CN^- ligands with a significant contribution from the Au(I) and Ag(I) centers. Regarding the final states, their contribution is mainly from the La(III) ions and the CN^- ligands. Nevertheless, it is important to note for the mixed systems that the most intense theoretical excitation for the Ag_2Au model system at 331.5 nm (oscillator strength = 0.0403) occurs between orbitals mainly located at Ag(I) centers and CN^- ligands to orbitals centered mainly at CN^- ligands with contribution from Au(I) and Ag(I) centers. Similarly, in the case of the $AgAu_2$ model system, one of the most important theoretical excitations at 329.9 nm (oscillator strength = 0.0350) takes place between occupied orbitals located at Au(I), Ag(I), and CN^- ligands and Au(I), Ag(I), and CN^--based orbitals. This feature would be qualitatively in accordance with the experimental observation in which the difference between the pure and the mixed systems comes from excited states delocalized over the Ag and Au centers for the latter as observed in the population analysis in which some virtual orbitals involved in the electronic excitations display delocalization between Au(I) and Ag(I) centers (see Supporting Information).

In conclusion, DFT calculations show a mixed character for the molecular orbitals. The occupied orbitals are mainly attributed to the CN^- ligands and to a small extent to Ag(I) and Au(I) metal centers. On the other hand, TD-DFT calculations as implemented in the software package used for this work (TURBOMOLE) permits the calculation of the theoretical absorption spectra. Thus, all the theoretical excitation spectra calculated in this work are comparable in energy with the corresponding experimental ones (not shown in the article).

TD-DFT calculations performed on the four model systems show some trends similar to those observed in the experimental emission spectra for the pure and mixed Au−Ag systems. For instance, the theoretical absorption energies for the mixed-model systems (Ag_2Au and $AgAu_2$) appear between the pure silver model (Ag_3), at higher energy, and the pure gold model (Au_3), at lower energy, as observed for the experimental luminescence measurements.

Finally, the assignment of the theoretical excitations responsible for the luminescent behavior is not easy. Anyway, in accord with the experimental assignment, it seems likely that the virtual orbitals involved in the absorption spectra in which the Ag(I) and/or Au(I) contribution is more important could be the ones involved in the emissive properties, with the rest being involved in nonradiative transitions. Furthermore, the long M(I)−M(I) interaction distances would suggest weaker interactions compared to already reported systems,[48] which makes the TD-DFT method appropriate to qualitatively explain some features of the photophysical properties of the $La[M(CN)_2]_3$ (M = Ag and/ or Au) systems.

Conclusion

Novel mixed-metal gold−silver lanthanide ion complexes have been synthesized and characterized using X-ray studies as well as Raman and luminescence spectroscopies. Heterometallic interactions between gold and silver have been observed from luminescence and Raman measurements. Interaction of the mixed-metal gold−silver ions have also been supported by electronic calculations. The mixed-metal compounds have a

Au−Ag Dicyanide Layered System Photoluminescence

J. Phys. Chem. B, Vol. 109, No. 10, 2005 **4323**

room-temperature intensity that is comparable to the low-temperature intensity, and this makes them promising for photoluminescence applications. Moreover they exhibit the characteristic properties of the pure Ag and Au compounds. Furthermore, the mixed-metal compounds can be tuned by varying the Ag:Au ratio. The mixed-metal compounds luminesce at an energy that lies between the emission bands of the pure Ag and Au compounds which is due to excited-state delocalization over the Ag and Au centers.

Note Added after ASAP Publication. There were errors in the fourth lanthanide complex in the Crystal Structures section and also in the third mixed-metal sample in the Luminescence Studies section in the version published ASAP February 11, 2005. The corrected version was published ASAP February 16, 2005.

Supporting Information Available: Tables of population analyses of single-metal and mixed-metal model systems and of theoretical excitations and oscillator strengths (pdf). This material is available free of charge via the Internet at http://pubs.acs.org.

References and Notes

(1) (a) Schmidbaur, H. *Gold Bull.* **1990**, *23*, 11. (b) Schmidbaur, H. *Chem. Soc. Rev.* **1995**, *24*, 391.

(2) (a) Pyykkö, P. *Chem. Rev.* **1997**, *97*, 597. (b) Pyykkö, P.; Zhao, Y.-F. *Angew. Chem., Int. Ed. Engl.* **1991**, *30*, 604. (c) Li, J.; Pyykkö, P. *Chem. Phys. Lett.* **1992**, *197*, 586. (d) Pyykkö, P.; Li, J.; Runeberg, N. *Chem. Phys. Lett.* **1994**, *218*, 133. (e) Pyykkö, P.; Runeberg, N.; Mendizabal, F. *Chem. Eur. J.* **1997**, *3*, 1451. (f) Pyykkö, P.; Mendizabal, F. *Chem. Eur. J.* **1997**, *3*, 1458.

(3) Leznoff, D. B.; Xue, B.-Y.; Batchelor, R. J.; Einstein, F. W. B.; Patrick, B. O. *Inorg. Chem.* **2001**, *40*, 6026.

(4) Fernández, E. J.; López-de-luzuriaga, J. M.; Monge, M.; Rodríguez, M. A.; Crespo, O.; Gimeno, M. C.; Laguna, A.; Jones, P. G. *Inorg. Chem.* **1998**, *37*, 6002.

(5) Assefa, Z.; Shankle, G.; Patterson, H. H.; Reynolds, R. *Inorg. Chem.* **1994**, *33*, 2187.

(6) (a) Rawashdeh-Omary, M. A.; Omary, M. A.; Patterson, H. H.; Fackler, J. P., Jr. *J. Am. Chem. Soc.* **2001**, *123*, 11237. (b) Rawashdeh-Omary, M. A.; Omary, M. A.; Patterson, H. H. *J. Am. Chem. Soc.* **2000**, *122*, 10371.

(7) (a) Rawashdeh-Omary, M. A.; Omary, M. A.; Shankle, G. E.; Patterson, H. H. *J. Phys. Chem. B.* **2000** *104*, 6143. (b) Rawashdeh-Omary, M. A.; Larochelle, C. L.; Patterson, H. H. *Inorg. Chem.* **2000**, *39*, 4527.

(8) Yersin, H.; Trümbach, D.; Strasser, J.; Patterson, H. H.; Assefa, Z. *Inorg. Chem.* **1998**, *37*, 3209.

(9) (a) Omary, M. A.; Patterson, H. H. *J. Am. Chem. Soc.* **1998**, *120*, 7696. (b) Patterson, H. H.; Kanan, S. M.; Omary, M. A. *Coord. Chem. Rev.* **2000**, *208*, 227.

(10) Omary, M. A.; Hall, D. R.; Shankle, G. E.; Siemiarczuk, A.; Patterson, H. H. *J. Phys. Chem. B* **1999**, *103*, 3845.

(11) Yersin, H.; Gliemann, G. *Ann. N. Y. Acad. Sci.* **1978**, *313*, 539.

(12) Gliemann, G.; Yersin, H. *Struct. Bonding (Berlin)* **1985**, *62*, 87.

(13) Cummings, S. D.; Eisenberg, R. *J. Am. Chem. Soc.* **1996**, *118*, 1949.

(14) (a) Colacio, E.; Lloret, F.; Kivekäs, R.; Suárez-Varela, J.; Sundberg, M.; Uggla, R.; *Inorg. Chem.* **2003**, *42*, 560. (b) Colacio E.; Lloret, F.; Kivekäs, R.; Ruiz, J.; Suárez-Varela, J.; Sundberg, M. *Chem. Commun.* **2002**, 592.

(15) Hoskins, B. F.; Robson, R.; Scarlett, N. V. Y. *Angew. Chem., Int. Ed. Engl.* **1995**, *34*, 1203.

(16) (a) Abrahams, S. C.; Bernstein, J. L.; Liminga, R. *J. Chem. Phys.* **1980**, *73*, 4585. (b) Abrahams, S. C.; Zyontz, L. E.; Bernstein, J. L. *J. Chem. Phys.* **1982**, *76*, 5458.

(17) (a) Leznoff, D. B.; Xue, B.-Y.; Patrick, B. O.; Sanchez, V.; Thompson, R. C. *Chem. Commun.* **2001**, 259. (b) Leznoff, D. B.; Xue, B.-Y.; Stevens, C. L.; Storr, A.; Thompson, R. C.; Patrick, B. O. *Polyhedron* **2001**, *20*, 2147.

(18) Yeung, W.-F.; Wong, W.-T.; Zuo, J.-L.; Lau, T.-C. *J. Chem. Soc., Dalton. Trans.* **2000**, 629.

(19) Shorrock, C. J.; Xue, B.-Y.; Kim, P. B.; Batchelor, R. J.; Patrick, B. O.; Leznoff, D. B. *Inorg. Chem.* **2002**, *41*, 6743.

(20) Ohba, M.; Okawa, H. *Coord. Chem. Rev.* **2000**, *198*, 313.

(21) Dunbar, K. R.; Heintz, R. A. *Prog. Inorg. Chem.* **1997**, *45*, 283.

(22) Vahrenkamp, H.; Geib, A.; Richardson, G. N. *J. Chem. Soc., Dalton Trans.* **1997**, 3643.

(23) (a) Viswanath, A. K.; Vetuskey, J.; Leighton, R.; Krogh-Jespersen, M.; Patterson, H. H. *Mol. Phys.* **1983**, *48*, 567. (b) Viswanath, A. K.; Patterson, H. H. *Chem. Phys. Lett.* **1981**, *82*, 25.

(24) Vosko, S. H.; Wilk, L.; Nusair, M. *Can. J. Phys.* **1980**, *58*, 1200.

(25) Perdew, J. P. *Phys. Rev. B* **1986**, *33*, 8822.

(26) Becke, A. D. *Phys. Rev. B* **1988**, *38*, 3098.

(27) Ahlrichs, R.; Bär, M.; Häser, M.; Horn, H.; Kölmel, C. *Chem. Phys. Lett.* **1989**, *162*, 165.

(28) Bauernschmitt, R.; Ahlrichs, R. *Chem. Phys. Lett.* **1996**, *256*, 454.

(29) Bauernschmitt, R.; Ahlrichs, R. *J. Chem. Phys.* **1996**, *104*, 9047.

(30) Bauernschmitt, R.; Häser, M.; Treutler, O.; Ahlrichs, R. *Chem. Phys. Lett.* **1997**, *264*, 573, and references therein.

(31) Gross, E. K. U.; Kohn, W. *Adv. Quantum Chem.* **1990**, *21*, 255.

(32) Casida, M. E. In *Recent Advances in Density Functional Methods*, Vol. 1; Chong, D. P., Ed,; World Scientific: Singapore, 1995.

(33) Olsen, J.; Jørgensen, P. In *Modern Electronic Structure Theory*, Vol. 2; Yarkony, D. R., Ed.; World Scientific: Singapore, 1995.

(34) Schäfer, A.; Horn, H.; Ahlrichs, R. *J. Chem. Phys.* **1992**, *97*, 2571.

(35) Dunning, T. H., Jr. *J. Chem. Phys.* **1994**, *100*, 5829.

(36) Andrae, D.; Haeussermann, U.; Dolg, M.; Stoll, H.; Preuss, H. *Theor. Chim. Acta* **1990**, *77*, 123.

(37) Colis, J. C. F.; Larochelle, C. L.; Staples, R.; Herbst-Irmer, R.; Patterson, H. H. *Dalton Trans.*, in press.

(38) Nyquint, R. A.; Putzig, M. A.; Leugers, M. A. In *The Handbook of Infrared and Raman Spectra of Inorganic Compounds and Organic Salts*, Vol. 2; Academic Press: San Diego, CA, 1997.

(39) Bottger, G. L. *Spectrochim. Acta* **1968**, *24A*, 1821.

(40) (a) Jones, L. H. *Spectrochim. Acta* **1963**, *19*, 1675. (b) Jones, L. H. *J. Chem. Phys.* **1957**, 26, 1578. (c) Jones, L. H. *J. Chem. Phys.* **1957**, *27*, 468. See also: Che, C. M.; Tse, M. C.; Chan, M. C. W.; Cheung, K. K.; Philips, D. L.; Leuung, K. H. *J. Am. Chem. Soc.* **2000**, *122*, 2464.

(41) Adams, D. M.; Fletcher, P. A. *Spectrochim. Acta* **1988**, *44A*, 437.

(42) Stammreich, H.; Chadwick, B. M.; Frankiss, S. G. *J. Mol. Struct.* **1967**, *1*, 191.

(43) (a) Larochelle, C. L. Ph.D. Thesis, Graduate School, University of Maine, 2001. (b) Colis, J. C. F. Ph.D. Thesis, Graduate School, University of Maine, 2004.

(44) Yersin, H.; Riedl, U. *Inorg. Chem.* **1995**, *34*, 1642, and references therein.

(45) Lee, Y.-L.; McGarrah, J. E.; Lachicotte, R. J.; Eisenberg, R. *J. Am. Chem. Soc.* **2002**, *124*, 10662.

(46) Nagasundaram, N.; Roper, G.; Biscoe, J.; Chai, J. W.; Patterson, H. H.; Blom, N.; Ludi, A. *Inorg. Chem.* **1986**, *25*, 2947.

(47) Sundholm, D. *Chem. Phys. Lett.* **2000**, *317*, 545.

(48) Fernández, E. J.; Gimeno, M. C.; Laguna, A.; López-de-Luzuriaga, J. M.; Monge, M.; Pyykkö, P.; Sundholm, D. *J. Am. Chem. Soc.* **2000**, *122*, 7287.